Bioprocess Engineering 11 (1994) 73–82 © Springer-Verlag 1994

A strategy to scale up nitrification processes with immobilized cells of nitrosomonas europaea and nitrobacter agilis

J. H. Hunik, J. Tramper, R. H. Wijffels

Abstract A scale-up strategy for a nitrification process with immobilized cells is presented. The complete description of such a process for a wide range of conditions is time consuming or even impossible. For a successful scale up of the process knowledge of the rate-limiting step is essential. To estimate the rate-limiting step a regime analysis was used. A new element in this regime analysis is a solid third phase in which cells grow non-homogeneously. Three different conditions of the nitrification process were considered: low temperature (7°C) with a low ammonia concentration (2 mM), and optimal temperature (30°C) with an ammonia concentration of 2 and 250 mM. The regime analysis proved to be a helpful tool for the understanding of the process and for establishing the rate-limiting step. A set of design rules for the different nitrification conditions was obtained from the results of this regime analysis.

List of symbols

a_g	$m^2 m^{-3}$ gas phase	specific surface area of a gas bubble
a_{lg}	$m^2 m^{-3}$ liquid phase	surface area of the liquid/gas inter phase
a_{ls}	$m^2 m^{-3}$ liquid phase	surface area of the solid/liquid inter phase
a_s	$m^2 m^3$ solid phase	specific surface area of a gelbead
d_b	m	gas bubble diameter
d_p	m	biocatalyst particle diameter
E_a	$J mol^{-1}$	activation energy
g	$m s^{-2}$	gravitational acceleration
H	$m^3 m^{-3}$	Henry coefficient
$\mathbb{D}$	$m^2 s^{-1}$	diffusion coefficient
k_{lg}	$m s^{-1}$	mass transfer coefficient for gas to liquid phase
k_{ls}	$m s^{-1}$	mass transfer coefficient for liquid to solid phase
K_S	$mol m^{-3}$	substrate affinity constant
m_s	mol N (kg biomassa)$^{-1}$ s^{-1}	maintenance coefficient
R	$J mol^{-1} K^{-1}$	gas constant
S	$mol m^{-3}$	substrate concentration
S_{sur}	$mol m^{-3}$	substrate concentration at surface of the biocatalyst
S_{bulk}	$mol m^{-3}$	substrate concentration in bulk phase
Y	$kg mol^{-1}$	yield coefficient for biomass on substrate
X	$kg m^{-3}$	biomass concentration
Z	dimensionless	temperature effected parameter value
z^{∞}	dimensionless	temperature independent parameter value
ε_g	m^3 gas m^{-3} liquid	gas hold up
ε_s	m^3 solid m^{-3} liquid	solid phase hold up
η^i	dimensionless	effectiveness factor
λ^i	$m^2 S mol^{-1}$	molar ionic conductivity
τ	s	characteristic time
τ_g	s	τ for growth
τ_{ex}^O	s	τ for oxygen exhaustion of gas bubbles
τ_{lg}^O	s	τ for oxygen transfer from gas to liquid phase
τ_{ret}^{liq}	s	τ for the liquid retention time
τ_{ret}^{gas}	s	τ for the gas retention time
τ_{ls}^i	s	τ for substrate (i) transfer from liquid to solid phase
τ_{mix}	s	τ for mixing of liquid phase
τ_{circ}	s	τ for liquid circulation in air-lift loop reactor
τ_{kin}^i	s	τ for substrate (i) conversion
τ_{conv}^i	s	τ for substrate (i) conversion in the biocatalyst
μ_{max}	s^{-1}	maximum specific growth rate
ω	$N s m^{-2}$	dynamic viscosity
ρ_l	$kg m^{-3}$	density of liquid phase
ρ_s	$kg m^{-3}$	density of solid phase
i		NH_4, NO_2^-, NO_3 and Ns, Nb for *N. europaea*, *N. agilis*, respectively.

Received 30 August 1993

J. H. Hunik, J. Tramper, R. H. Wijffels
Department of Food Science, Food and Bioprocess Engineering Group, Agricultural University, Wageningen, P.O. box 8129, 6700 EV Wageningen, The Netherlands

This project was supported by the European Community in the programme Science and Technology for Environmental Protection (ref. STEP-CT91-0123).

1 Introduction

Problems related to the discharge of nitrogen compounds into the environment are topical nowadays. Both diluted

wastestreams such as sewage and more concentrated wastestreams like manure contribute to nitrogen-related environmental problems. For example, discharges of ammonia from various sources have a considerable effect on algal blooms in the North Sea [40]. The removal of ammonia with biological nitrification is a widely used process in wastewater treatment. The active-sludge process with biomass retention gives a considerable ammonia removal in diluted waste streams (2–5 mM NH_4^+) at moderate temperatures (15–25°C). Nitrification in an active-sludge process is, however, limited by a slow growth of the two main bacterial species involved: *Nitrosomonas spp.* and *Nitrobacter spp.* This growth-rate limitation is most severe at unfavourable conditions like, for example, lower temperatures [16, 24, 25] or concentrated wastestreams where inhibition of substrate and product are important [2].

Immobilization of nitrifying bacteria can be a successful strategy to handle biomass-retention problems [23]. Several immobilization methods are applied. For example, at low temperatures rotating biological contactors are used by Gullicks and Cleasby [7] and by Murphy et al. [20], and immobilization of pure cultures in κ-carrageenan gels by Leenen et al. [18] and by Wijffels et al. [35]. Also for manure treatment rotating biological contactors are applied [29].

Most of the research on nitrification focuses on small-scale experiments and extensive modelling of immobilized nitrifying bacteria. Several dynamic models for immobilized nitrifying bacteria are presented and validated [5, 6, 12, 33, 36]. Large-scale applications of this immobilized-cell process are limited to a few plants because this complicated process is difficult to scale up [10]. A better understanding of the rate-limiting factors, important for scaling up, can be obtained with a regime analysis [31]. From such a regime analysis a set of design directives for the different applications of immobilized nitrifying bacteria can be derived.

Air-lift loop reactors are most suitable for immobilized-cell processes. They lack mechanical stirring and are each to scale up. Mechanical stirring can cause abrasion of the immobilization material and should therefore be avoided. Air-lift loop reactors are characterized, among others, by Verlaan [32] and Chisti [4] with respect to their liquid circulation, mixing properties and mass transfer.

The regime analysis presented here is based on an air-lift loop reactor design for a nitrification process with immobilized cells. The existing theory for regime analysis was extended with cells growing non-homogeneously in gel beads. Reactor performance and other information necessary for the regime analysis were simulated with a dynamic model [12]. The regime analysis was used to derive the rate-limiting step and design directives for three cases of the nitrification process with immobilized cells: low temperature (7°C) with low ammonia concentration (2 mM), and optimal temperature (30°C) with an ammonia concentration of 2 and 250 mM.

2 Theory

2.1 Regime analysis

A system with immobilized cells for nitrification has a complex behaviour. A complete description of the process for a wide range of conditions is time consuming or even impossible. This argument is valid for most biotechnological processes and a consistent approach to simplify these processes is regime analysis [19, 27]. In the regime analysis presented by Schouten et al. [28], with immobolized *Clostridium spp.* for isopropanol/butanol production, the effectiveness factor for the immobilized cells was estimated to be 1. They conclude that the isopropanol/butanol production is not diffusion controlled and the immobilized cells behave as free cells. New for the regime analysis presented here is the addition of a solid third phase with immobilized cells growing in a diffusion-controlled situation.

Regime analysis can either be used for the optimization of the reactor design or to reveal the rate-limiting step of a process, see Fig. 1 [31]. Optimization of the reactor design requires several iterations until a previously defined optimum is obtained. Here we are interested in the rate-limiting step of the process and not in optimization of the reactor design. The regime analysis starts with an inventory of all transport and conversion mechanisms of the process. The characteristic time of each mechanism is then estimated; relatively slow mechanisms have a high characteristic time, while lower characteristic times apply to faster mechanisms. The comparison of characteristic times for conversion and transport mechanisms of a particular substrate can thus reveal the rate-limiting step.

For nitrification with cells non-homogeneously growing in a gel bead several transport mechanisms for the substrates (O_2 and NH_4^+), intermediate (NO_2^-) and product (NO_3^-) can be distinguished: mass transfer of oxygen from air bubbles to the liquid phase; mass transfer of oxygen and ammonia from the bulk phase to the gel beads; mass transfer of oxygen, ammonia and nitrite within the beads to the cells, and mass transfer of nitrite (intermediate) and nitrate (product) from the beads to the liquid. All these transport mechanisms are characterized with either a mass-transfer coefficient or a diffusion coefficient. The conversion is characterized by the substrate consumption rate. This chain of transport and conversion should be combined with the reactor characteristics in the actual regime analysis. Mixing, circulation, gas and liquid retention times should be compared with the characteristic times for transport and conversion to reveal if gradients in the reactor bulk phase can be expected.

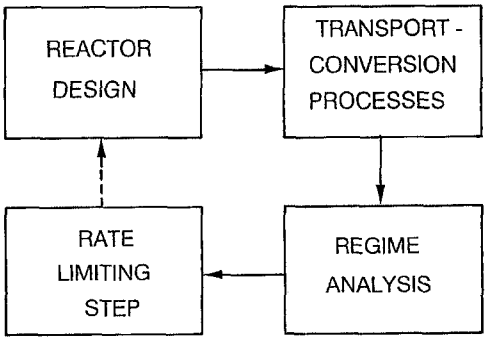

Fig. 1. Regime analysis

2.2 Characteristic times

Examples of relations for characteristic times are found in the literature [5, 19, 31]. In general these relations are obtained from the ratio between a capacity and a flow:

$$\tau = \frac{\text{capacity}}{\text{flow}}. \quad (1)$$

Capacity is defined as the available substrate for transport or conversion at process conditions. The flow is the rate of that particular transport or conversion. The characteristic time for mixing and circulation, which have already time as dimension, are directly used in the regime analysis.

When regime analysis is used for a three-phase system one phase must be used as a sort of "pivot" for the characteristic-time calculations. Most convenient is the continuous (liquid) phase, which is therefore, unless mentioned otherwise, used as "pivot" phase for the characteristic-time definitions given below.

The characteristic time (τ_{lg}^{O}) for the mass transfer of oxygen from the gas phase to the liquid phase is given by

$$\tau_{lg}^{O} = \frac{1}{k_{lg} * a_{lg}}, \quad (2)$$

with k_{lg} as gas–liquid mass-transfer coefficient [m s^{-1}] and a_{lg} as the gas-surface area per unit of liquid volume [m^2 m^{-3}]. The latter is given by

$$a_{lg} = a_g \frac{\varepsilon_g}{1-\varepsilon_g}, \quad (3)$$

with ε_g as the gas hold up [m^3 gas m^{-3} liquid] and a_g as the specific surface area of the gas phase per unit of gas volume [m^2 m^{-3}] based on d_b, the gas bubble diameter [m]:

$$a_g = \frac{6}{d_b}. \quad (4)$$

Transport of oxygen from the gas bubble to the liquid phase depletes the gas bubbles of oxygen. The characteristic time for the gas-bubble oxygen exhaustion (τ_{ex}^{O}) is given by

$$\tau_{ex}^{O} = \frac{H}{k_{lg} * a_g}, \quad (5)$$

with the H as the Henry coefficient [m^3 liquid m^{-3} gas]. The τ_{ex}^{O} in Eq. (5) is based on the gas phase, because the depletion of this phase is considered here.

The characteristic time (τ_{ls}) for the mass transfer from the liquid to the solid phase is given by

$$\tau_{ls} = \frac{1}{k_{ls} * a_{ls}}, \quad (6)$$

with k_{ls} as the liquid–solid mass transfer coefficient [m s^{-1}] and a_{ls} as the solid-surface area per unit of liquid volume [m^2 m^{-3}]. The latter is given by

$$a_{ls} = a_s \frac{\varepsilon_s}{1-\varepsilon_s}, \quad (7)$$

with ε_s as the solid hold up [m^3 solid m^{-3} liquid] and a_s as the specific surface area of the solid phase per unit of solid volume [m^2 m^{-3}] based on d_p the gel bead diameter [m]:

$$a_s = \frac{6}{d_p}, \quad (8)$$

Characteristic times for liquid circulation, mixing and gas-phase retention time in air-lift loop reactors are related to the size of the reactor. The mixing time (τ_{mix}) for an air-lift loop reactor is calculated from the circulation time (τ_{circ}) as shown by Verlaan [32]:

$$\tau_{mix} = (4 \text{ to } 7) \cdot \tau_{circ}. \quad (9)$$

This value of τ_{circ} can be measured easily in an existing reactor or calculated for a given reactor design [32].

The maximum gas-phase-retention time (τ_{ret}^{gas}) in an air-lift loop reactor is calculated from the ratio of the reactor height and terminal rising velocity (approximately 0.25 m/s [8]) of the gas bubbles. The actual value for gas-phase retention time (τ_{ret}^{gas}) will be shorter when liquid circulation in the loop reactor is taken into account. The liquid-retention time (τ_{ret}^{liq}) is the reciprocal value of the dilution rate.

The characteristic time τ_{kin} for the substrate conversion by free cells is derived from the biomass concentration X [kg m^{-3}], the substrate concentration S [mol m^{-3}], and the kinetic parameters K_s [mol m^{-3}], Y [kg mol^{-1}], and μ_{max} [s^{-1}] of the relevant microorganism [27]:

$$\tau_{kin} = \frac{S}{\left[\frac{\mu_{max} * X}{Y}\right]\left[\frac{S}{K_S + S}\right]}. \quad (10)$$

When we consider solid gel beads with immobilized cells and if all the cells in these gel beads "feel" the substrate concentration at the surface (S_{sur}), Eq. (10) will reduce to

$$\tau_{kin} = \left[\frac{Y}{\mu_{max} * X}\right](K_S + S_{sur}), \quad (11)$$

with X expressed as kg m^{-3} gel.

The situation inside the gel beads is more complicated because substrate and biomass concentrations vary with the radius of the gel bead. It is not possible to define an overall characteristic time for transport or conversion in such a situation. To circumvent this problem we introduce the internal effectiveness factor which is defined as the ratio between the observed conversion rate (actual flow) and the conversion rate which would be observed if all the biomass would "feel" the substrate concentration at the surface of the gel beads (flow for S_{sur} [26]). In this effectiveness factor both transport and conversion are taken into account. For the calculation of the effectiveness factor it is important to realize that the observed conversion rate of the cells in the gel beads (actual flow) is equal to the flow of substrate from the bulk to the gel-bead surface. This liquid to solid mass-transfer rate is substituted in the definition for the actual flow in the internal effectiveness factor (η), which yields

$$\eta = \frac{k_{ls} * a_{ls} * (S_{bulk} - S_{sur})}{\left[\frac{\mu_{max} * X}{Y}\right]\left[\frac{S_{sur}}{K_S + S_{sur}}\right]}. \quad (12)$$

The value for the effectiveness factor approaches 0 for a strictly transport-controlled process and 1 for a completely

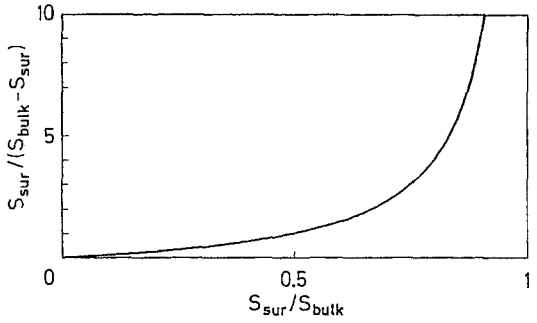

Fig. 2. Relation between S_{sur} and S_{bulk} with respect to solid/liquid mass transfer and conversion rate of the biocatalyst in Eqs. (6) and (13)

kinetically controlled process. With η going from 1 to 0, the relative conversion rate decreases and the corresponding characteristic time increases. Therefore, τ_{kin} and the reciprocal value for η were combined in Eq. (13) to derive a characteristic time for substrate conversion by in immobilized cells (τ_{conv}). This results in a ratio between capacity (S_{sur}) and actual flow of substrate to the gel beads (denominator of Eq. (13)), which is exactly the definition of a characteristic time (Eq. (1)) for the overall substrate conversion by the gel beads (τ_{conv}):

$$\tau_{conv}=\frac{S_{sur}}{k_{ls}*a_{ls}*(S_{bulk}-S_{sur})}. \tag{13}$$

The substrate concentration at the surface of the gel beads (S_{sur}) is the key value, which determines the relative importance of the liquid-solid mass transfer and the conversion by the immobilized cells. This can be illustrated by taking the ratio of Eqs (6) and (13) yielding a relation between the characteristic time for liquid-solid mass transfer and substrate conversion in the gel beads

$$\frac{\tau_{conv}}{\tau_{ls}}=\frac{S_{sur}}{S_{bulk}-S_{sur}}. \tag{14}$$

The effect of S_{sur} on the ratio of the characteristic time for substrate conversion (τ_{conv}) and solid-liquid mass transfer (τ_{ls}) is shown in Fig. 2. This figure shows that with a surface concentration of half that of the bulk concentration, the characteristic times τ_{kin} and τ_{conv} are equal. Two extreme situations can be distinguished in Fig. 2. First, when S_{sur} is 0 the conversion is completely controlled by liquid-solid mass transfer. Second, for S_{sur} is equal to S_{bulk}, the conversion is completely kinetically controlled. The surface concentration (S_{sur}) of the biocatalyst is not easy to measure, but can be estimated from experimental results or model predictions [12].

3
Process description

Three different cases for the nitrification process with immobilized cells were considered in the regime analysis: Nitrification at low temperature (7°C) with a low ammonia concentration of 2 mM (LTLA), nitrification in an extreme environment of ammonia (250 mM) and an optimal temperature of 30°C (OTEE), and nitrification at optimal temperature (30°C) and low ammonia concentration of 2 mM (OTLA). The latter was taken as the reference for the two other cases. A dynamic model (Hunik et al. [12]) was used to simulate the nitrification process for these three cases. The original model uses parameter values based on a temperature of 30°C, but incorporation of the effects of lower temperatures on these model parameters are described here.

3.1
Model

The dynamic model consists of a set of transport and kinetic equations for the conversion of ammonia via nitrite to nitrate with immobilized *Nitrosomonas europaea* and *Nitrobacter agilis* cells in an air-lift loop reactor. The dynamic character of the model allows changes in reactor cases. The growth of cells and the concentration of substrate, intermediate and product together with biomass concentrations for *N. europaea* and *N. agilis* are predicted as a function of the gel-bead radius. The model input consists of a set of parameters obtained from independent experiments together with the initial values for biomass concentrations, reactor set-up and experimental cases like temperatures and influent concentrations. For the regime analysis the model was used to predict the conversion capacities and the S_{sur} value for the three nitrification cases considered. The parameters used for the model are shown in Table 1. A more detailed description of the model is given by Hunik et al. [12]. The parameters for gas-liquid transport (H, d_b, k_{lg}) necessary for the regime analysis are obtained from Heijnen and Riet [8] and also shown in Table 1.

3.2
Temperature T influence on parameters

The optimal temperature for nitrification is around 30°C and parameters used in the model of Hunik et al. [12] are based on this temperature. Knowledge of the temperature influence on the model parameters is necessary for the simulations at 7°C. This temperature influence can be expressed with an Arrhenius type of equation:

$$Z^T=z^{\infty}\exp\left(\frac{-E_a}{R*T}\right), \tag{15}$$

with Z^T the parameter value at temperature T, z^{∞} as a constant, E_a [J mol^{-1}] as the activation energy and R [J mol^{-1}K^{-1}] as the gas constant.

3.3
Influence of T on the maximum specific growth rate

For the determination of the activation energy (E_a) for the growth rate of *Nitrosomonas europaea* and *Nitrobacter agilis* experimental data given in several literature sources [11, 14, 30] were used. In Fig. 3a, b the μ_{max} values given in these sources for both microorganisms are plotted as function of temperature. In these figures the fits of Eq. (15) for the various sets are also drawn. The E_a values used in this study for the two microorganisms are averages of the values obtained from the 3 sets. These average E_a values are 65 and 45 kJ mol^{-1} for *N. europaea* and *N. agilis*, respectively. The z^{∞} values are obtained from substitution of the average E_a values and the values for μ_{max} at 30°C from Table 1 in Eq. (15). The resulting equation is used for calculating μ_{max} values at 7°C. With this procedure we obtained μ_{max} values of 1.9×10^{-6} and 2.3×10^{-6} s^{-1} for *N. europaea* and *N. agilis*, respectively, at 7°C.

Table 1. Model parameters

Parameter	Value at 30°C Hunik et al. [12]	Value at 7°C	Dimension
Conversion			
μ_{max}^{Ns}; μ_{max}^{Nb}	1.59×10^{-5}; 1.0×10^{-5}	1.9×10^{-6}; 2.3×10^{-6}	s^{-1}
m_s^{Ns}; m_s^{Nb}	9.4×10^{-4}; 2.2×10^{-3}	2.6×10^{-4}; 6.4×10^{-4}	mol N (kg biomass)$^{-1}$ s^{-1}
Y^{Ns}; Y^{Nb}	1.66×10^{-3}; 0.58×10^{-3}	1.66×10^{-3}; 0.58×10^{-3}	(kg biomass) mol N^{-1}
$K_S^{NH_4, Ns}$	1.25×10^{-3}	1.16×10^{-4}	mol dm^{-3}
$K_S^{O_2, Ns}$	5.05×10^{-6}	9.3×10^{-7}	mol dm^{-3}
$K_S^{NO_2, Nb}$	3.6×10^{-4}	2.5×10^{-5}	mol dm^{-3}
$K_S^{O_2, Nb}$	17.0×10^{-6}	3.1×10^{-6}	mol dm^{-3}
$I_{NO_2}^{Nb}$, $I_{NO_3}^{Nb}$	0.159; 0.188		mol dm^{-3}
Transport gas–liquid			
$k_{lg}(O_2)$	4.4×10^{-4}	2.7×10^{-4}	m s^{-1}
H	39	25	$m^3 m^{-3}$
d_b	6×10^{-3}	6×10^{-3}	m
Transport liquid–solid			
k_{ls} N-comp; O_2	2.65×10^{-5}; 3.13×10^{-5}	1.41×10^{-5}; 1.75×10^{-5}	m s^{-1}
d_p	2×10^{-3}		m
ε_s	0.25		dimensionless
ω	8.4×10^{-4}	1.66×10^{-3}	N $s m^{-2}$
$\mathbb{D}_w$ N-comp; O_2	2.2×10^{-9}; 2.83×10^{-9}	1.1×10^{-9}; 1.55×10^{-9}	$m^2 s^{-1}$
$\mathbb{D}_{gel}$ N-comp; O_2	1.9×10^{-9}; 2.05×10^{-9}	1.0×10^{-9}; 1.2×10^{-9}	$m^2 s^{-1}$

3.4 Influence of T on the substrate-affinity constants

Little information about the effect of temperature on the affinity constants of O_2, NH_4^+ and NO_2^- is available in the literature. In fact three studies were found [1, 14, 15]. The E_a values found in these three literature sources were used with the substrate affinity values of Table 1 at 30°C to substitute in Eq. (15) in order to obtain the values for z^∞. Boon and Laudelout [1] measured an E_a of 52 kJ mol^{-1} for the affinity constant of oxygen ($K_S^{O_2, Nb}$) with *N. winogradskyi* (z^∞: 1.57×10^7 mol m^{-3}). Laudelout & van Tichelen [15] obtained an E_a value of 82 kJ mol^{-1} for the affinity constant NO_2^- ($K_S^{NO_2, Nb}$) also for *N. winogradskyi* (z^∞: 4.92×10^{13} mol m^{-3}). From the data of Knowles et al. [14] we obtained an E_a of 73 kJ mol^{-1} for the NH_4^+ affinity constant ($K_S^{NH_4, Ns}$) of a mixed culture (z^∞: 4.82×10^{12} mol m^{-3}). For the missing E_a value of the affinity constant of oxygen for *E. europaea* ($K_S^{O_2, Ns}$) we used 52 kJ mol^{-1} which is the same value as the affinity constant of oxygen for *N. winogradskyi.* This latter value is also used by Laudelout et al. [17] for *N. europaea.* (z^∞: 4.65×10^6 mol m^{-3}). The substrate affinity constants at 7°C are estimated with this z^∞ and E_a values.

3.5 Influence of T on maintenance and yield

The effect of temperature on the maintenance (m_s) of a large number of aerobic microorganisms is described y Heijnen and Roels [9]. They found an activation energy (E_a) of 38 kJ mol^{-1} for the maintenance of all aerobic microorganisms. The m_s at 7°C calculated with this E_a and maintenance values at 30°C of Table 1 was 2.6×10^{-4} and 6.4×10^{-4} mol N kg^{-1} s^{-1} for *N. europaea* and *N. agilis*, respectively. Concerning biomass yield, in the literature survey of Heijnen and Roels [9] it can be read that the biomass yield (Y) is independent of T.

3.6 Influence of T on the dynamic viscosity

Equation (15) was fitted to the data of the dynamic viscosity (ω) of water [34]. A value of 6.021×10^{-7} N s m^{-2} and 18.1 kJ mol^{-1} was obtained for z^∞ and E_a, respectively.

3.7 Influence of T $\mathbb{D}$ of O_2 and nitrogen compounds

The influence of temperature on the diffusion coefficient of oxygen in water is given by Wise and Houghton [39]. A value of 4.2×10^{-6} $m^2 s^{-1}$ and 18.4 kJ mol^{-1} for respectively z^∞ and E_a are given. For the diffusion coefficient of oxygen in the gel beads, Wijffels et al. [37] obtained a value of 19×10^{-6} $m^2 s^{-1}$ for z^∞ and 17.2 kJ mol^{-1} for E_a.

Diffusion coefficients of NH_4^+ and NO_2^- and NO_3^- in water and biofilms at different temperatures are scarcely found. Therefore,
it was not possible to estimate the E_a and z^∞ values. The diffusion coefficients for these nitrogen compounds in water and biofilms at 7°C were therefore estimated using the temperature dependency of the dynamic viscosity (ω) with the following relation [21]:

$$\mathbb{D}(T_1)\frac{\omega(T_1)}{T_1} = \mathbb{D}(T_2)\frac{\omega(T_2)}{T_2}. \quad (16)$$

The diffusion coefficients at 7°C thus estimated are 1.1×10^{-9} and 1.0×10^{-9} $m^2 s^{-1}$ for water and biofilm, respectively.

3.8 Influence of T on gas–liquid mass transfer

The mass-transfer coefficient for oxygen at the gas liquid interphase is a rather empirical parameter. Influence of bubble size and media composition are difficult to take into account. A value of 4×10^{-4} m s^{-1} at 20°C with a temperature

dependency of 2.5% increase per °C is used by Heijnen and Riet [8]. For the gas liquid mass-transfer coefficient (k_{lg}) at 7°C and 30°C a value of 2.7×10^{-4} and 4.4×10^{-4} m s^{-1} respectively, were estimated based on this temperature relation. The Henry coefficient (H) for oxygen is 39 [m^3 gas m^{-3} liquid] at 30°C and 25 [m^3 gas m^{-3} liquid] at 7°C [13].

3.9
Influence on T on liquid–solid mass transfer

For the mass-transfer coefficient of the liquid–solid interphase an estimation is possible, based on the film-theory. This mass-transfer coefficient depends on the dynamic viscosity and on the diffusion coefficient, which are both temperature dependent. For the mass-transfer coefficient we assume, based on the similar values for the diffusion coefficient, one value for the three nitrogen compounds. For both temperatures it is possible to calculate the mass-transfer coefficient k_{ls} [36]. For that, a value of 1000 and 1008 kg/m^3 is used for the density of water and gel beads, respectively.

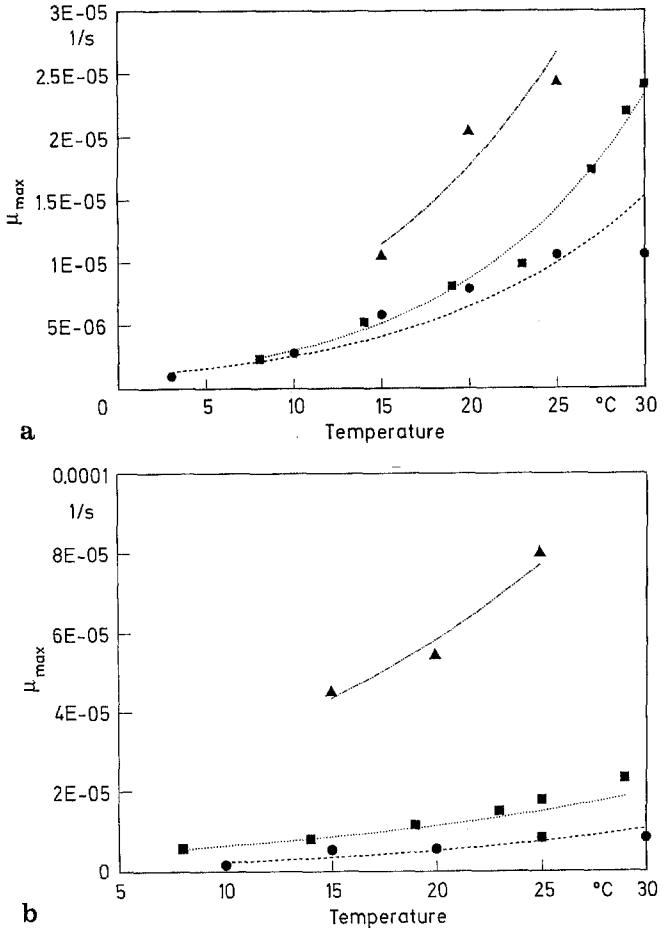

Fig. 3a, b. The maximum rate of a *Nitrosomonas spp.* and b *Nitrobacter spp.* as a function of temperature. Symbols are the measured values, lines are based on Eq. (15) fitted to these values, with - - - ● - - - [11], ... ■ .... [14] and — · ▲ —·— [30]

3.10
Design and initial values for the model

A nitrification process at a low temperature of 7°C in, for example, Norway should have a capacity of 2×10^4 m^3 day^{-1} with an ammonia concentration in the waste water of 2 mM [22]. This implies an ammonia conversion rate of 4×10^4 mol N day^{-1}. From this capacity and some initial trials with the model we derived the reactor volumes and dilution rates for all three cases considered here.

The prerequisite of the design was an ammonia conversion at steady state of 75% for the low ammonia cases (LTLA and OTLA) and 95% for the extreme environment case (OTEE). The reactor dimensions, dilution rates, temperatures and influent concentrations are shown in Table 2.

The model input value for the initial biomass concentration of *N. europaea* and *N. agilis* are the same as used by Hunik et al. [12], i.e. 4×10^{-3} and 2×10^{-4} kg/m^3 gel, respectively. The maximum biomass concentration in the model was set at 8.9 and 3.8 kg/m^3 gel for *N. europaea* and *N. agilis*, respectively. These values are identical to the values of Hunik et al. (1993). A 50 day run of the model was sufficient to reach a steady-state conversion rate of ammonia and nitrite for the three processes. The temperature for the LTLA process was taken 30°C for the first ten days of the experiment; for the rest of the experiment the temperature was set at 7°C. The optimal temperature of 30°C during the start-up phase was used to accelerate the biomass formation. A steady-state conversion of ammonia within a 50 day run could be achieved with such an increased start-up temperature. The final concentration of 250 mM NH_4^+ in the OTEE process was reached by starting with 50 mM and subsequently increasing it to 100 mM at day 6, 150 mM at day 15, 200 mM at day 25 and finally 250 mM NH_4^+ at day 35. This step-wise increase was used to avoid the inhibitory effect of NO_2^- in the start-up phase.

4
Results and discussion

For the three nitrification process cases considered, model simulations generated the bulk-phase concentrations of NH_4^+, NO_2^- and NO_3^- and these are shown in Fig. 4a–c as a function of time. The decrease in NH_4^+ concentration and the production of

Table 2. Reactor design

Reactor	Volume	Dilution rate	Influent	Temperature
	[m^3]	[s^{-1}]	NH_4^+ [mM]	°C
Low temperature (LTLA)	833	2.8×10^{-4}	2	7
Optimal temperature (OTLA)	278	8.3×10^{-5}	2	30
Extreme environment (OTEE)	514	3.9×10^{-6}	250	30

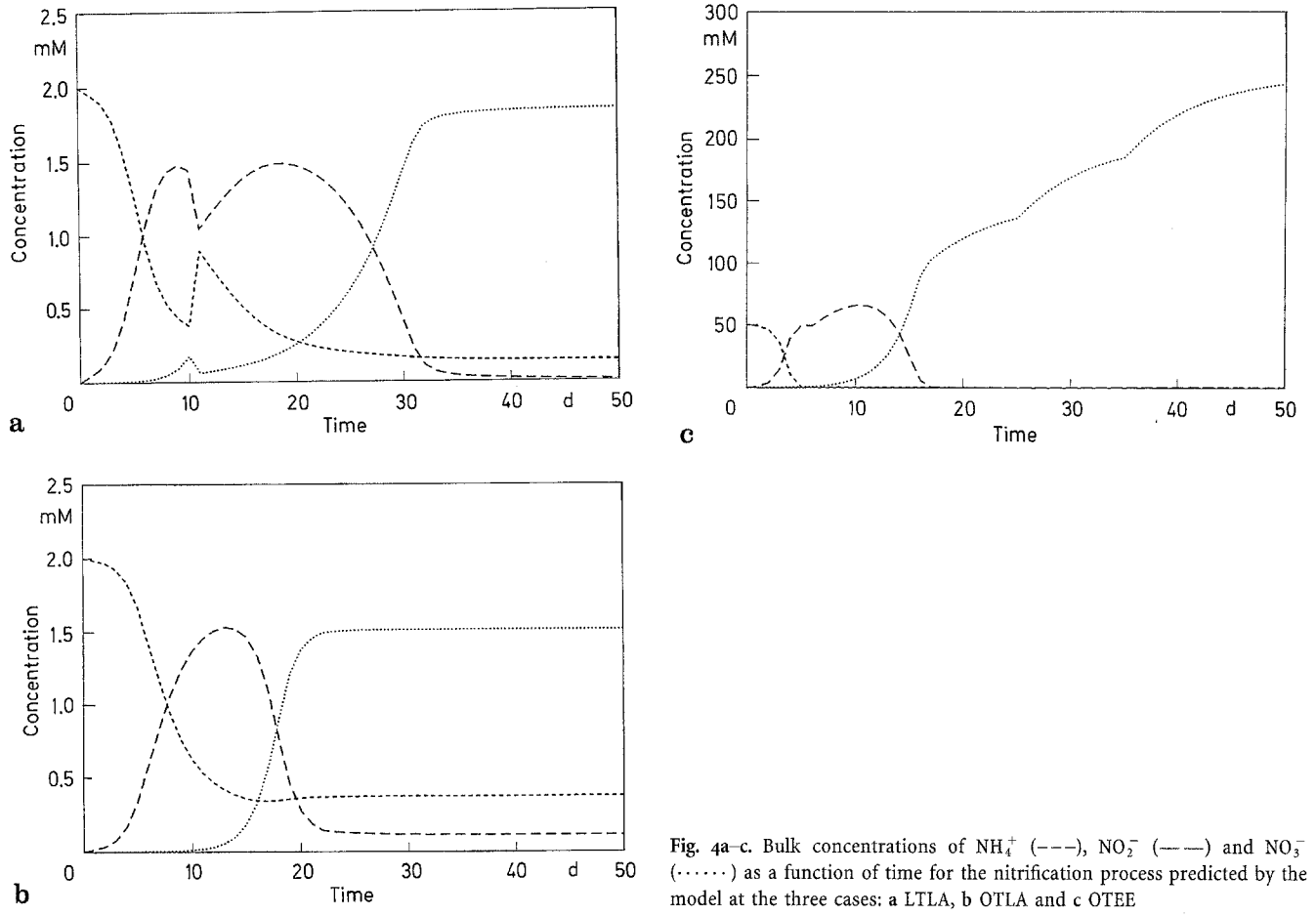

Fig. 4a–c. Bulk concentrations of NH_4^+ (– – –), NO_2^- (— —) and NO_3^- (· · · · · ·) as a function of time for the nitrification process predicted by the model at the three cases: a LTLA, b OTLA and c OTEE

NO_2^- during the first 10 days was caused by the growth of *N. europaea*. The production of NO_3^- and the related growth of *N. agilis* start between day 10 and 20 depending on the process cases. The reactor concentrations of the OTLA case are shown in Fig. 4b. The temperature step at day 10 for the LTLA case is observed in Fig. 4a. The step-wise increase in influent ammonia concentration in the OTEE case resulted in a step-wise increase in nitrate concentration as shown in Fig. 4c. The criteria for the nitrification capacity, at least 75% ammonia removal for the low ammonia cases (LTLA and OTLA) and more then 95% for the high ammonia concentration case (OTEE), were satisfied for all three nitrification cases. The presented data of the model simulations were used in the regime analysis.

4.1
Regime analysis

The values for the gas-phase hold up (ε_g) and liquid mixing time (τ_{mix}) depend on the reactor configuration and size. Gas hold up (ε_g) values for air-lift loop reactors will be in the range of 0.02–0.05 [4, 32]. Riet and Tramper [26] present some data about circulation and mixing times in air-lift loop reactors based on the model of Verlaan [32]. The mixing (180–600 s) and circulation times (45–150 s) they present are for two external air-lift loop reactors with a volume of 265 and 1227 m^3, respectively, a height to riser diameter ratio of 10:1 and a ratio between the riser to downcomer diameter of 2:1. A difference between mixing and circulation time should be made for loop reactors. Mixing times are useful for pulse-wise addition of a substrate to the reactor and circulation times are more useful for continuous addition of substrates in loop reactors. This latter situation is more applicable and circulation times were therefore used to predict gradients in the reactors.

The characteristic times for all the transport mechanisms in the reactor are independent of the substrate concentrations. This is in contrast to the characteristic time of substrate conversion (τ_{conv}), which depends on the surface concentration of the gel bead. This surface concentration decreased during the start up and finally reached a steady state. The course of τ_{conv} for the three cases is shown in Fig. 5a–c. The regime analysis is based on the steady-state values reached after 50 days model simulation. The characteristic times for conversion and transport are presented in Table 3 and discussed below with respect to the substrate involved.

4.2
Oxygen

Oxygen depletion of the gas phase depends on the mass transfer of oxygen from gas to liquid phase and amount of oxygen available in the gas phase. With the values for $\tau_{ex}^{O_2}$ and τ_{ret}^{gas} (Table 3) we can conclude that complete exhaustion of the gas bubble is not likely to happen, but a significant decrease in oxygen concentration in the gas bubble will occur. Oxygen exhaustion

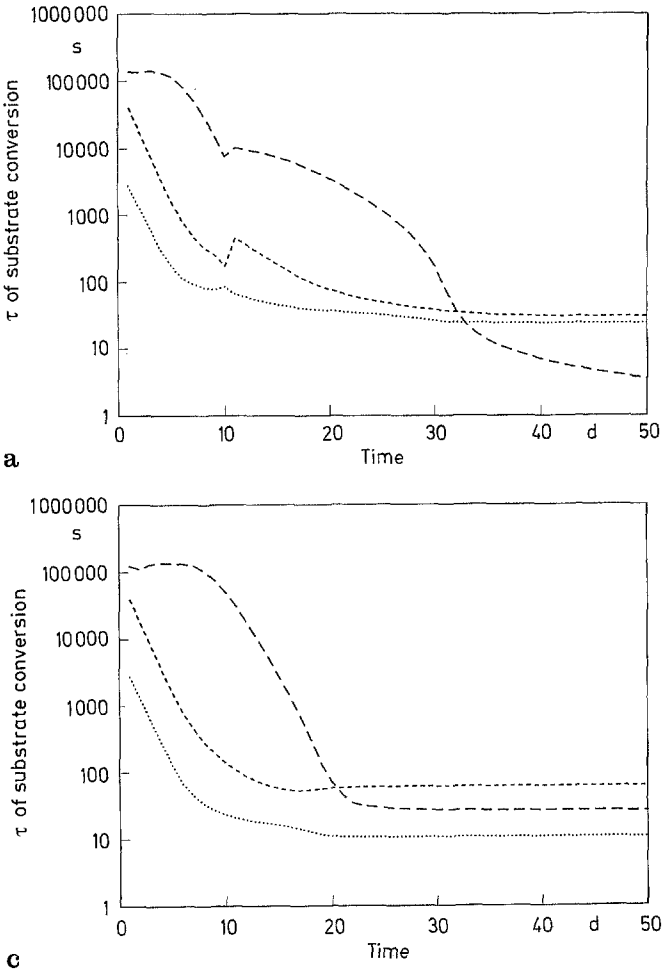

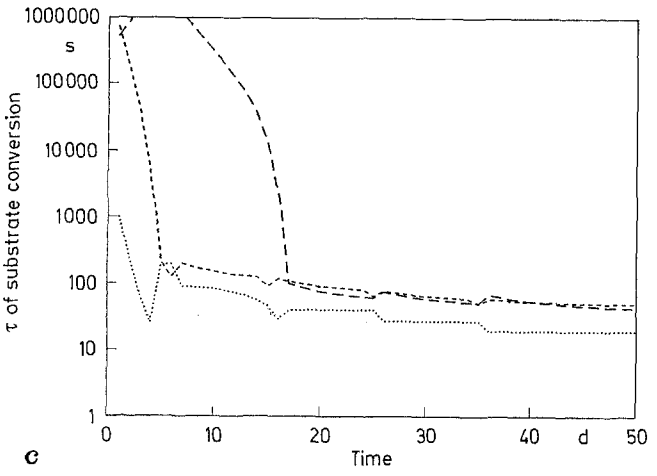

Fig. 5a–c. The characteristic time for substrate conversion (τ_{conv}) of the three substrates, NH_4^+ (- - - -) and NO_2^- (— —) and O_2 (. . . .) as a function of time for the nitrification process at three different cases a LTLA, b OTLA and c OTEE. Values are obtained from model simulations

Table 3. Characteristic times of transport and conversion processes for the three nitrification processes. The τ_{conv} values are based on the steady-state values at day 50 in Fig. 5a–c

	Characteristic time (τ) [s]		
Transport phenomena	LTLA (7°C)	OTLA (30°C)	OTEE (250 mM)
τ_{gas}^{ret}	20	20	20
$\tau_{ex}^{O_2}$	93	78	78
$\tau_{lg}^{O_2}$ ($\varepsilon_g = 0.02$–0.05)	181–70	98–38	98–38
$\tau_{ls}^{O_2}$	57	35	35
τ_{liq}^{ret}	3600	1200	2.6×10^5
$\tau_{ls}^{NH_4}$	71	42	42
τ_{circ}	40–150	40–150	40–150
Conversion processes			
$\tau_{conv}^{NH_4}$	30	61	50
$\tau_{conv}^{NO_2}$	3.5	26	43
$\tau_{conv}^{O_2}$	24	11	19

of gas bubbles in air-lift loop reactors does not become important beneath a reactor height of 15 m, but it also depends on the liquid velocity in the riser.

Oxygen is transported from gas phase via the liquid phase to the solid phase. The rate of this transport is determined by the characteristic times for gas-liquid mass transfer ($\tau_{lg}^{O_2}$), liquid-solid mass transfer ($\tau_{ls}^{O_2}$) and oxygen conversion ($\tau_{conv}^{O_2}$). In Table 3 the values for $\tau_{lg}^{O_2}$ (at $\varepsilon_g = 0.05$), $\tau_{ls}^{O_2}$ and $\tau_{conv}^{O_2}$ are in the same order of magnitude and only trends can thus be indicated. The differences in characteristic times are not sufficient to indicate one step in the process as the only rate-limiting step.

The values for $\tau_{lg}^{O_2}$ (at $\varepsilon_g = 0.05$), $\tau_{ls}^{O_2}$ and $\tau_{conv}^{O_2}$ are decreasing in this order. The fastest process is the oxygen conversion and the higher values for $\tau_{lg}^{O_2}$ and $\tau_{ls}^{O_2}$ indicate that transport of oxygen from the gas phase to the gel beads is likely to be rate limiting. With a lower gas hold up (at $\varepsilon_g = 0.02$) the value for $\tau_{lg}^{O_2}$ increases and mass-transfer resistance will even be more important. This

is particularly the case for the OTLA case with the lowest value for $\tau_{conv}^{O_2}$.

The liquid circulation time (τ_{circ}) is in the same order of magnitude as the characteristic times for gas-liquid mass transfer ($\tau_{lg}^{O_2}$) and liquid-solid mass transfer ($\tau_{ls}^{O_2}$). Gradients in O_2 concentration in the liquid phase can thus be expected. A gel bead, when circulating through the loop reactor, will encounter rapid changes in O_2 concentrations as a consequence of this gradients.

4.3 Ammonia and nitrite

The situation for NH_4^+ is restricted to the liquid and solid phase. The liquid phase can be assumed well mixed with respect to NH_4^+ because liquid retention time (τ_{ret}^{liq}) is large compared to the circulation time (τ_{circ}). The characteristic time for NH_4^+ conversion by the immobilized *N. europaea* cells ($\tau_{conv}^{NH_4}$) is of the same order of magnitude as that for mass transfer ($\tau_{ls}^{NH_4}$) between liquid and solid phase. The rate of conversion of NH_4^+ will thus be controlled by both the liquid–solid mass transfer and NH_4^+ conversion by the immobilized cells.

Nitrite is produced within the gel beads by the *N. europaea* cells and mass transfer between liquid and solid phase of NO_2^- is thus not important. The value of $\tau_{conv}^{NO_2}$ for the LTLA case is an order of magnitude smaller than the value for $\tau_{conv}^{NH_4}$. This indicates that nitrite conversion is a faster process compared to ammonia conversion and accumulation of NO_2^- is not likely to happen for the LTLA case. This is in contrast with the OTLA and OTEE case where the value of $\tau_{conv}^{NO_2}$ is close to the value for $\tau_{conv}^{NH_4}$. The NO_2^- and NH_4^+ conversion rates are well balanced for the OTLA and OTEE case and distortion of this balance can cause accumulation of NO_2^-. High values for the concentration of toxic NO_2^- in the effluent of a nitrification process are obviously unacceptable.

4.4 Nitrification

The regime analysis shows that the nitrification process is mainly controlled by mass transfer of the two substrates and to a lesser extent by the conversion rates of them. Accumulation of nitrite is possible at optimal temperature and very unlikely at low temperature. The characteristic time of the NH_4^+ conversion for both the OTLA and OTEE case is considerably longer than that for O_2 conversion. The nitrification for both the OTLA and OTEE is controlled by the O_2 transport and to lesser extent by its conversion.

4.5 Design rules

Regime analysis shows that nitrification with immobilized cells is mainly controlled by mass transfer of oxygen. This is an improvement compared to the active sludge process, which is controlled by the slower process of bacterial growth. The design for the OTLA and OTEE case can be further improved with respect to oxygen transport, in particular between gas and liquid phase. This oxygen transport is dependent of k_{lg}, a_{lg}, k_{ls} and a_{ls}. Smaller gas bubbles and gel beads increase these values of k_{lg}, a_{lg}, k_{ls} and a_{ls}. The relation between a_{ls} and gel bead diameter (d_p) is shown in Eqs. (7) and (8). A decrease in gel bead diameter (d_p) would increase the value a_{ls}. Nevertheless, the minimum gel bead diameter (d_p) is limited by the requirement to keep the gel beads in the reactor. The gas bubble diameter (d_b) is determined by the sparger and the coalescence behaviour of the medium, which is difficult to manipulate. For this reason, it is not useful to produce small bubbles in a coalescent medium because, the advantage of the small bubbles disappears short after the sparger. An increase in gas hold up (ε_g) would be beneficial for the oxygen-transfer rate according to Eq. (3). An increase of solid phase hold up (ε_s), i.e. more gel beads in the reactor, is limited to a maximum of 35%, and the k_{lg} will be reduced [32]. For the design of the LTLA case the gas–liquid mass transfer of both oxygen and ammonia could be improved by smaller gel beads and a slightly higher solid-phase hold up.

Sufficient liquid mixing, e.g. prevention of oxygen gradients, should be provided for in all three nitrification processes with immobilized cells. Oxygen gradients in the reactor can be decreased when the retention time in the non-aerated downcomer is short and the overall circulation time is kept as small as possible. Reactors should therefore have a relatively high riser to downcomer diameter ratio and small height to diameter ratio.

The ratio of *N. europaea* and *N. agilis* biomass concentrations is particular important for the optimal temperature processes and can be controlled with the inoculum size during immobilization. This biomass ratio is not important for the LTLA process, because the growth rate of *N. agilis* decreases less with a decrease of temperature than the growth rate of *N. europaea*.

References

1. **Boon, B.; Laudelout, H.:** Kinetics of nitrite oxidation by *Nitrobacter winogradskyi*. Biochem. J. 85 (1962) 440–447
2. **Bortone, G.; Piccinini, S.:** Nitrification and denitrification in activated-sludge plants for pig slurry and wastewater from cheese diaries. Bioresource Technol. 37 (1991) 243–252
3. **Brian, P. T. L.; Hales, H. B.:** Effects of transpiration and changing diameter on heat and mass transfer to spheres. A.I.Ch.E. J. 15 (1969) 419–425
4. **Chisti, M. Y.:** Airlift bioreactors. England, Essex: Elsevier 1989
5. **Gooijer, C. D. de; Wijffels, R. H.; Tramper, J.:** Growth and substrate consumption of *Nitrobacter agilis* cells immobilized in carrageenan: Part 1. dynamic modeling. Biotechnol. Bioeng. 38 (1991) 224–231
6. **Gujer, W.; Boller, M.:** A mathematical model for rotating biological contactors. In: Proc. of the technical advances in bioreactors conference, Nice, pp 69–89. Paris, CFRP-AGHTM 1989
7. **Gullicks, H. A.; Cleasby, J. L.:** Cold-climate nitrifying biofilters: design and operation considerations. J. WPCF 62 (1990) 50–57
8. **Heijnen, J. J.; Riet, K. van't:** Mass transfer, mixing and heat transfer phenomena in low viscosity bubble column reactors. Chem. Eng. J. 28 (1984) B21–B42
9. **Heijnen, J. J.; Roels, J. A.:** A macroscopic model describing yield and maintenance relationships in aerobic fermentation processes. Biotechnol. Bioeng. 23 (1981) 739–763
10. **Heijnen, J. J.; Mulder, A.; Weltevrede, R.; Hols, J.; Leeuwen, H. L. J. M. van:** Large scale anaerobic-aerobic treatment of complex industrial waste water using biofilm reactors. Water Sci. Technol. 23 (1991) 1427–1436
11. **Helder, W.; Vries, R. T. P. de:** Estuarine nitrite maxima and nitrifying bacteria (Ems-Dollard estuary). Netherlands J. Sea Res. (in English) 17 (1983) 1–18
12. **Hunik, J. H.; Bos, C. G.; Hoogen, M. P. van den; Gooijer, C. D. de; Tramper, J.:** Validation of a dynamic model for substrate conversion and growth of Nitrosomonas europaea and *Nitrobacter agilis* cells immobilized in κ-carrageenan beads. Biotechnol. Bioeng. (accepted for publication)
13. **Janssen, L. P. B. M.; Warmoeskerken, M. M. C. G.:** Fysisch technologisch bij-de-hand boek. Delft, The Netherlands: DUM 1982
14. **Knowles, G.; Downing, A. L.; Barrett, M. J.:** Determination of kinetic constants for nitrifying bacteria in mixed culture, with the aid of electronic computer. J. Gen. Microbiol. 38 (1965) 263–278

15. **Laudelout, H.; Tichelen, L. van:** Kinetics of the nitrite oxidation by *Nitrobacter winogradskyi.* J. Bact. 79 (1960) 39–42
16. **Laudelout, H.; Lambert, R.; Fripiat, J. L.; Pham, M. L.:** Effet de la température sur la vitesse d'oxydation de l'ammonium en nitrate par des cultures mixtes de nitrifiants. Ann. Microbiol. (Inst Pasteur) 125B (1974) 75–84
17. **Laudelout, H.; Lambert, R.; Pham, M. L.:** Influence du pH et la pression partielle d'oxygène sur la nitrification. Ann Microbiol (Inst Pasteur) 127A (1976) 367–382
18. **Leenen, E. J. T. M.; Englund, G.; Tramper, J.; Wijffels, R. H.:** Effluent treatment at low temperatures using artificially immobilized nitrifying bacteria, In: Proc. int. conf. on Sewage into 2000, Part 2: Wastewater treatment, pp. 339–350. Amsterdam, IAWPRC/EWPCA/NVA 1992
19. **Moser, A.:** Bioprocess technology: kinetics and reactors. New York, USA: Springer 1988
20. **Murphy, K. L.; Sutton, P. M.; Wilson, R. W.; Jank, B. E.:** Nitrogen control: design considerations for supported growth systems. J. WPCF 49 (1977) 549–557
21. **Neumann, J. S.:** Electrochemical systems. Englewood Cliffs, NJ: Prentice-Hall 1973
22. **Ødegaard, H.; Paulsrud, B.; Bilstad, T.; Pettersen, J. E.:** Norwegian strategies in the treatment of municipal wastewater towards the reduction of nutrient discharges to the North Sea. In: North Sea pollution, technical strategies for improvement, pp. 355–366. Amsterdam, The Netherlands: IAWPRC/EWPCA/NVA 1990
23. **Okey, R. W.; Albertson, O. E.:** Diffusion's role in regulating rate and masking temperature effects in fixed-film nitrification. J. WPCF 61 (1989) 500–509
24. **Painter, H. A.:** Nitrification in the treatment of sewage and waste-waters. In: Prosser, J. I. (Ed.): Nitrification: Special publications of the society for general microbiology, vol. 20, pp. 185–211. Oxford, UK: IRL Press 1986
25. **Randall, C. W.; Buth, D.:** Nitrite build-up in activated sludge Resulting from temperature effects. J. WPCF 56 (1984) 1039–1044
26. **Riet, K. van't; Tramper, J.:** Basic bioreactor design. New York, USA: Marcel Dekker Inc. 1991
27. **Roels, J. A.:** Energetics and kinetics in biotechnology. Amsterdam, The Netherlands: Elsevier Biomedical Press 1983
28. **Schouten, G. H.; Guit, R. P.; Zieleman, G. J.; Luyben, K. Ch. A. M.; Kossen, N. W. F.:** A comparative study of a fluidized bed reactor and a gas lift loop reactor for the IBE process: Part 1. reactor design and scale down approach. J. Chem. Technol. Biotechnol. 36 (1986) 335–343
29. **St-Arnaud, S.; Bisaillon, J.-G.; Beaudet, R.:** Microbiological aspects of ammonia oxidation of swine waste. Can. J. Microbiol. 37 (1991) 918–923
30. **Stratton, F. E.; McCarty, P. L.:** Prediction of nitrification on the dissolved oxygen balance of streams. Current Res. 1 (1967) 405–410
31. **Sweere, A. P. J.; Luyben, K. Ch. A. M.; Kossen, N. W. F.:** Regime analysis and scale-down: tools to investigate the performance of bioreactors. Enzyme Microbiol Technol. 9 (1987) 386–398
32. **Verlaan, P.:** Modelling and characterization of an airlift-loop reactor, Ph.D. Thesis, Wageningen Agricultural University, The Netherlands 1987
33. **Wanner, O.; Gujer, W.:** A multispecies biofilm model, Biotechnol. Bioeng. 28 (1984) 314–328
34. **Weast, R. C.; Astle, M. J. (Eds.):** CRC handbook of chemistry and physics, 60th edition, pp. F51. Boca Raton, FL: CRC Press Inc. 1980
35. **Wijffels, R. H.; Hunik, J. H.; Gooijer, C. D. de; Tramper, J.:** Nitrification with immobilized bacteria in airlift loop reactors; modelling and application. In: Christiansen, C.; Munck, L.; Villadsen, J. (Eds): Proc. of the 5th European congress on biotechnology, pp. 392–395. Copenhagen, Denmark 1990
36. **Wijffels, R. H.; Gooijer, C. D. de; Kortekaas, S.; Tramper, J.:** Growth and substrate consumption of *Nitrobacter agilis* immobilized in carrageenan: Part 2. Model evaluation. Biotechnol. Bioeng. 38 (1991) 232–240
37. **Wijffels, R. H.; Englund, G.; Hunik, J. H.; Leenen, E. T. J. M.; Bakketun, Å.; Günther, A.; Obón de Castro, J. M.; Tramper, J.:** Effects of diffusion limitation on immobilized nitryfying organisms at low temperature. (submitted)
38. **Williamson, K.; McCarty, P. L.:** Verification studies of the biofilm model for bacteria substrate utilization. J. WPCF 48 (1976) 281–296
39. **Wise, D. L.; Houghton, G.:** The diffusion of ten slightly soluble gases in water at 10–60°C. Chem. Eng. Sci. 21 (1966) 999–1010
40. **Zevenboom, W.; Rademaker, M.; Colijn, F.:** Exceptional algal blooms in dutch north sea waters. In: North Sea pollution, technical strategies for improvement, pp. 473–486. IAWPRC/EWPCA/NVA, Amsterdam, The Netherlands 1990